Unusual lyotropic polymorphism of deoxyguanosine-5'-monophosphate: X-ray diffraction analysis of the correlation between self-assembling and phase behavior

Hermann Franz,* Federica Ciuchi, Giovanni Di Nicola, Monica M. De Morais, and Paolo Mariani†
Istituto di Scienze Fisiche, Università degli Studi di Ancona, Via Ranieri 65, 60131 Ancona, Italy
(Received 14 July 1993)

The concentration-temperature dependent phase diagram of the deoxyguanosine-5'-monophosphate [d(pG)]–water system was determined by x-ray diffraction measurements. The columnar lyotropic polymorphism has been confirmed. However, at medium concentrations and high temperatures, we found an unusual and large region of coexistence of isotropic and hexagonal phases (maybe in equilibrium with the cholesteric phase). Increasing the ionic strength of the solution by adding KCl, resulted in a stabilization of the high-temperature hexagonal phase and a direct isotropic to hexagonal (with increasing concentration) and a cholesteric to hexagonal (with increasing temperature) phase transition were observed. The phase diagrams completely agree with the one predicted for hard rod-shaped particles. In order to understand the phase behavior, the cholesteric and hexagonal unit cell parameters were analyzed at different temperatures as a function of the volume concentration of d(pG) on the basis of recent statistical-mechanical calculations. Moreover, by analyzing the high-angle [$s=(3.4\ \text{Å})^{-1}$] peak, the average number of coherently scattering tetramers was also determined. For d(pG) in pure H_2O, we obtained values between 35 and 53. After adding KCl, the functional dependence turned out to be more complex, and we obtained values between 26 and 58.

PACS number(s): 61.30.−v, 64.70.Md, 61.10.Lx, 87.15.By

I. INTRODUCTION

Of the five nucleotides found in DNA and RNA, only guanosine shows the ability to self-associate into stable structures. This phenomenon is well known: ordered gels and fibers from guanosine, 5'- and 3'-guanosine monophosphate, polyguanosine and deoxyguanosine have been studied extensively [1–4]. The common basic building block of such structures has been found to be a planar disk-shaped quartet (the so-called tetramer) formed by four Hoogsteen-bonded guanosine moieties [4,5]. The tetrameric arrangement of the four guanosines is represented in Fig. 1. Recently, naturally single-stranded sequences from telomers and other chromosomal locations have been found to form a family of higher-order structures *in vitro* (the so-called quadriplexes): these include structures containing guanine quartets bonded together according to the Hoogsteen hydrogen-bonding scheme [6]. The possible biological relevance of this guanine special feature is, as yet, undefined: it has been proposed that the formation of the quadriplex mediates the parallel pairing of the four homologous chromatids during meiosis and the dimerization of the telomeric ends of chromosomes [6–9], and may have a prebiotic significance in the origin of the genetic code [10].

In recent papers [11–13], we have reported that a series of guanosine derivatives show, at room temperature and as a function of water concentration, a columnar lyotropic liquid crystalline polymorphism. In particular, we observed that the ammonium salt of the nucleoside phosphate 2'-deoxyguanosine-5'-monophosphate d(pG), as well as the sodium salts of the corresponding "dimer" 2'-deoxyguanylyl-(3'-5')-2'-deoxyguanosine d(GpG), of the "trimer" d(GpGpG), of the "tetramer" d(GpGpGpG) and of the "hexamer" d(GpGpGpGpGpG), are able to self-associate in water to form hexagonal (*H*) and cholesteric (Ch) mesophases at low and high water content, respectively [11–13]. On the basis of x-ray diffraction and optical microscopy experiments [12–14], we demonstrated that these liquid crystalline phases are

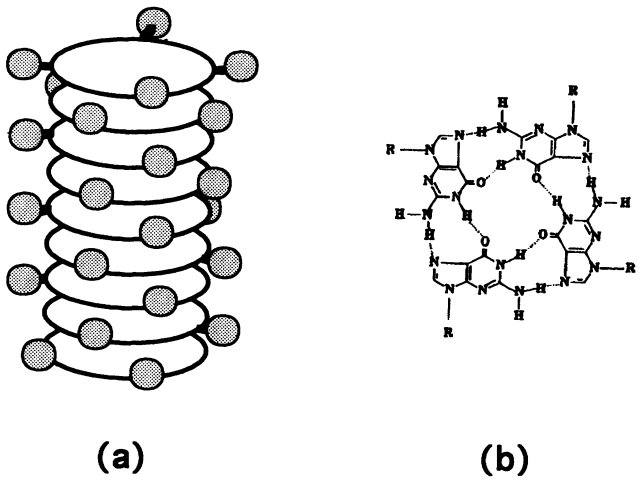

FIG. 1. Schematic representation of the microscopic structure of d(pG) aggregates. (a) Stacking of the disk-shaped tetramers. The spherical legands symbolize the residual sugar groups (*R*). (b) In-plane structure of one tetramer.

*Present address: Physik Department E13, Technische Universität München, James-Franck-Strasse 1, D-85748 Garching, Germany.
†Author to whom correspondence should be addressed.

formed by chiral, cylindrical aggregates with negative diamagnetic anisotropy and that each rod is composed of a stacked array of tetrameric disks at the typical distance of 3.4 Å (see again Fig. 1). Moreover, except in an overly diluted d(pG) sample, short four-stranded aggregates of similar structure were also observed in the isotropic solutions by small-angle neutron-scattering experiments [15]. In particular, for weight concentrations of 1% and 1.5%, and irrespective with the "distance" from the isotropic-cholesteric (*I*-Ch) phase transition concentration, cylindrical aggregates of 13 Å radius and about 65 Å length were detected. Recently, a more complex columnar polymorphism was identified in the ammonium salt of 2'-deoxyguanosine-3'-monophosphate d(Gp) and in its isobutyl ester d(Gp)iBu [16]. Due to steric constraints and strong short-range intercolumnar interactions, these compounds show, as a function of water concentration, four different columnar phases, including a cholesteric and a hexagonal phase, but also a two-dimensional square and a new hexagonal H_b structure [16].

Another important feature, defined by several works on various guanosine-containing systems [17,18] and stressed by recent circular dichroism experiments [19], is that those four-stranded structures specifically need alkali metal cations in order to form. Moreover, depending on the nature of the alkali cations, the structure of the aggregates appears differentially stabilized. This effect, which is not clearly defined, as kinetic and thermodynamics mechanisms seem to competitively control the self-assembling process in solution, could be roughly explained in terms of a size-selective binding of cations within the central cavity of the tetramers.

On the basis of these results and in order to obtain further information on the self-association properties of guanosine, we decided to investigate extensively by x-ray diffraction methods the polymorphic behavior of the 2'-deoxyguanosine-5'-monophosphate ammonium salt as a function of temperature and ionic strength (i.e., in the presence and absence of excess K^+ ions).

II. EXPERIMENTAL DETAILS

d(pG) was of commercial origin (Sigma, 99% purity). Samples were prepared by mixing the guanosine derivative with freshly bidistilled water. To study the influence of the ionic strength of the solution, we also investigated samples in 4*M* KCl. The mixtures were left for at least two days at room temperature to avoid inhomogeneity. After mounting the sample holder, the homogeneity of the samples was verified by optical polarizing microscopy. The relative uncertainty of the concentrations was estimated to be 5%. Concentrations are reported as weight fraction, c, or volume fraction, c_v, as appropriate. Volume concentrations have been calculated using for d(pG) the specific volume 0.651 cm^3/g.

Low-angle x-ray diffraction experiments were performed using a 1.5 kW Ital-Structures x-ray generator equipped with a Guinier-type focusing camera operating in vacuum: a bent quartz crystal monochromator was used to select the Cu $K\alpha_1$ radiation ($\lambda = 1.54$ Å). The samples were mounted in vacuum-tight cells with thin mica windows. In order to reduce the spottiness arising from possible macroscopic monodomains, the cells were continuously rotated during exposure. The sample cell temperature was controlled with an accuracy of 0.5 °C by using a circulating thermostat. The diffraction patterns were recorded on a stack of four Kodak DEF-392 films. Scattering data were also recorded on a two circle diffractometer equipped with a bent position sensitive detector (INEL CPS120) to record the scattered intensity in a range of $\Delta 2\theta = 120°$ at the same time. A Philips PW1830 was used as x-ray source, run at a power of 1.6 kW with a copper target. The Cu $K\alpha_1$ line was selected by a Guinier monochromator focused on the detector. The intrinsic resolution of the diffractometer (width of a crystalline peak) was determined to be 1.1 channels. The width of one channel was measured using a LiF single crystal and calculated to be 0.0300(2)°.

III. RESULTS

In this work, the structural properties of d(pG) in water and in 4*M* KCl have been investigated. The phase sequence of d(pG) at 25 °C in pure water was already established in [13]. In particular, as a function of concentration, an isotropic, a cholesteric and a hexagonal phase were observed. The present x-ray scattering analysis, which confirms at 25 °C the same sequence also for d(pG) in 4*M* KCl, is focused in particular on the high temperature region of the two phase diagrams.

As a typical example for the scattering cross section (SCS) observed in these systems, Fig. 2 shows the x-ray diffraction profiles observed at 75 °C and 25 °C for d(pG) in 4*M* KCl with $c = 0.40$. In Fig. 2(a), two low-angle peaks (order $+1$ and -1) related to the two-dimensional hexagonal lattice are easily identified. Using the Guinier camera, we were able to identify also higher order reflexions—up to the fifth order in some cases—as published in [13]. However, no extra low-angle peaks were observed in this phase, indicating the absence of smectic-like order. As expected, in fact, no long-range column-column correlation of the tetramer position exists, as the rods may freely translate in a direction perpendicular to the two-dimensional hexagonal cell. The scattering pattern observed at low temperature is reported in Fig. 2(b): the liquid crystalline phase shows lower symmetry and it is assumed to be cholesteric, as confirmed by optical microscopy. The peaks of the ordered phase have transformed to broad bands, whose maxima are hardly visible with the resolution obtained with the diffractometer, but were clearly resolved by using the Guinier camera. In both Figs. 2(a) and 2(b), the high-angle peaks related to the stacking of the tetramers may be seen. The corresponding scattering vector s [$s = (2\sin\theta)/\lambda$] confirmed the distance of 3.4 Å between the piled tetramers and thus the columnar model described above. The x-ray diffraction profiles relative to the isotropic phase are not shown: they are characterized by diffuse scattering in the small-angle region and by the absence of the high-angle peak.

In the following, we present in more detail our results regarding those two characteristic features. First, the

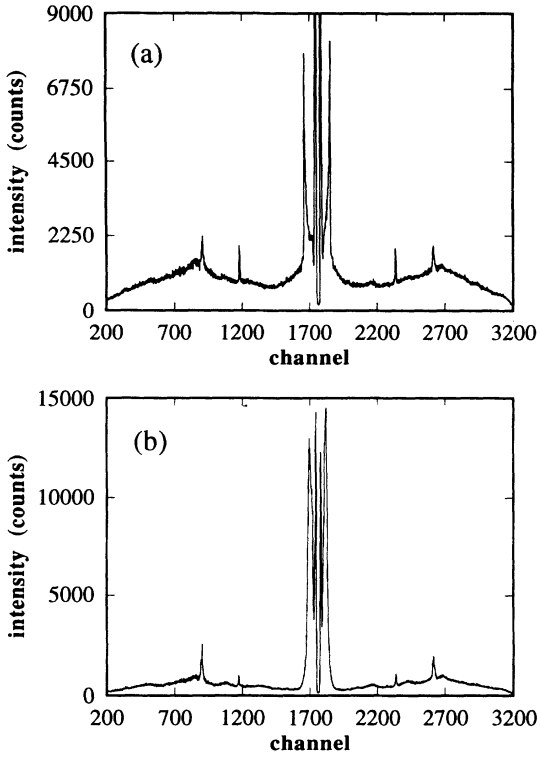

FIG. 2. As recorded x-ray intensities of d(pG) 40% in 4*M* KCl. (a) 75 °C; (b) 25 °C. The direct beam (centered at channel 1779) is blocked by a beamstop. In the low-angle region, the peaks due to the liquid crystalline order are observed. The asymmetry is due to smearing effects. In the high-angle region, the peaks reflecting the stacking of the tetramers are located near the maximum of the structure factor of H_2O. The peaks near channels 1150 and 2300 are due to the mica windows.

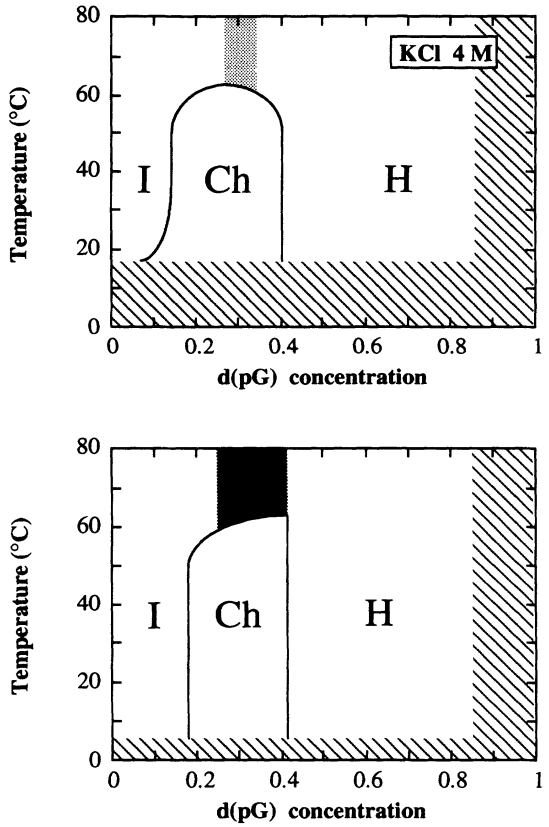

FIG. 3. Phase diagrams of d(pG)-H_2O (lower frame) and d(pG)–4*M* KCl (upper frame) as deduced from our measurements (concentrations in relative weight). *I*, isotropic, Ch, cholesteric, and *H*, hexagonal phases. Shaded region: phase coexistence. The lines give the positions of the phase transitions, the width of which was determined to be below 5%. In the hatched areas, we have no measured data.

low-angle scattering, reflecting the liquid crystalline phases and their transitions, and second, the high-angle profile, containing information on the columnar aggregation of the tetramers.

A. Phase diagrams of d(pG)

From the analysis of the low-angle scattering region recorded at different temperatures and concentrations, the phase diagrams of d(pG) in H_2O and in 4*M* KCl have been derived (see Fig. 3). In the first phase diagram, we observe at medium concentration and low temperature a region of cholesteric stability, while the isotropic and the hexagonal phases coexist at high temperature. The extension of this two-phase domain appears considerably reduced after addition of KCl: a direct cholesteric to hexagonal phase transition with increasing temperature is, in fact, observed at concentrations near 40%. Noticeable is the fact that in both systems the triple point temperature remains unchanged at about 60 °C. However, in 4*M* KCl, the cholesteric phase extends to far lower concentrations, whereas the Ch to *H* phase transition appears only slightly shifted towards lower concentrations.

The general features of both phase diagrams are in agreement with recently published ones, calculated on the basis of a hard-particle model [20] or for persistent flexible rods [21]. In the case of completely rigid aggregates, Taylor and Herzfeld [20] obtain for weak aggregation (i.e., when the average aggregate size is small) a direct isotropic-hexagonal phase transition with increasing amphiphile concentration. However, for sufficiently strong aggregation (i.e., when the aggregates are on average sufficiently elongated), they find a stable nematic phase, intervening between the isotropic and the columnar phase. In the case of persistent flexible hard rods, Hentschke and Herzfeld [21] derive for moderate flexibility an isotropic-nematic-hexagonal phase sequence with increasing amphiphile concentration. By contrast, as the rods become more flexible, they find that the isotropic-to-nematic transition shifts to higher concentrations, until finally a direct isotropic-to-columnar phase transition occurs. On the basis of such theoretical results, we can interpret the observed phase diagrams considering the d(pG) system as formed either by rigid and reversibly assembled rodlike aggregates, with average size increasing with increasing concentration and with decreasing temperature, or by hard rodlike aggregates of fixed length, with flexibility increasing with increasing temperature.

B. Unit cell dimensions

In Fig. 4, the hexagonal unit cell parameter a and the mean distance between adjacent cylinders in the cholesteric phase, as calculated from the position of the low-angle peaks observed for d(pG) in H_2O, are plotted at four different temperatures as a function of volume concentration c_v. As expected, we found a monotonic decrease of the unit cell dimensions with increasing concentration. The same behavior was observed in the KCl containing system, the only difference being that the unit cell dimensions in both cholesteric and hexagonal phases are larger (about 8–10 %) than the ones observed at the same concentration and temperature in pure water.

As recently reported [14,22], it is useful to extensively investigate the dependence of a on the d(pG) volume concentration. However, due to similar behavior, we restricted the detailed study to the case of d(pG) in H_2O. Let us begin by assuming that the four-stranded columns in the hexagonal phase are infinitely long and have a circular section with radius R. The relation between the cross-sectional area of the rod and the two-dimensional hexagonal unit cell surface is [12,13,23]:

$$\pi R^2=(\sqrt{3/2})a^2c_v \ .$$

In the present system, R could be considered constant as the structure and conformation of the disk-shaped tetramer does not change as a function of concentration [1,24]. Therefore, for infinite cylinders, a will change with volume concentration as $c_v^{-1/2}$:

$$a=(2\pi R^2/\sqrt{3})^{1/2}c_v^{-1/2} \ .$$

This means that the rods move apart only laterally as dilution proceeds. Moreover, on the basis of theoretical calculations [20,21], see also Ref. [22], a power law dependence for the variation of the dimensions of the hexagonal unit cell with volume concentration has been predicted for monodisperse spherocylinders of fixed length, with short-range repulsions only. In these calculations, the flexibility of the aggregates, which are considered to homogeneously bend elastic along their contour, plays an important role (see also Ref. [25]). The theory distinguishes between spherocylinder length regimes relative to a flexibility persistence length, which is a measure of the distance over which the orientations of two unit vectors tangential to the free columnar aggregate contour are correlated [21,25]. Exponents of $-\frac{1}{3}$ and $-\frac{1}{2}$ are predicted for spherocylinders that are rigid (shorter than the persistence length) and flexible (longer than the persistence length), respectively [20,21]. For monodisperse rigid spherocylinders that grow in length with increasing concentration, the theoretical equation for the hexagonal lattice dimension indicates that the exponent will be greater than $-\frac{1}{3}$.

Straight lines corresponding to $-\frac{1}{2}$ and $-\frac{1}{3}$ power law behaviors are then shown in Fig. 4. For low temperatures (5 °C and 25 °C), the data points are aligned fairly well on the curve for infinite (or finite flexible) aggregates. At 40 °C, there is a crossover from the infinite (or finite flexible) to the finite rigid type behavior at the H to Ch phase transition (note, however, that the above indicated theory was derived for the hexagonal phase, so that its extension to a nematic phase is entirely hypothetical). Finally, at high temperature, the data points in the H phase vary even slower than $c_v^{-1/3}$. Note that in the two-phase region the lattice dimensions remain fairly constant. Comparing the different temperatures, the negative lateral, thermal expansion predicted by [20] is demonstrated in our measurements. The relevance of those results for the microscopic model of the polymorphism will be discussed in the following section.

C. Aggregation of tetramers

The columnar stacking of the tetramers may be studied in more detail analyzing shape and position of the high-angle [$s=(3.4\ \text{Å})^{-1}$] peak. To do this, we fitted a Gaussian and a locally linear background to every peak (see Fig. 5). The results are summarized in Figs. 6 and 7: the first figure shows the distance between the positions

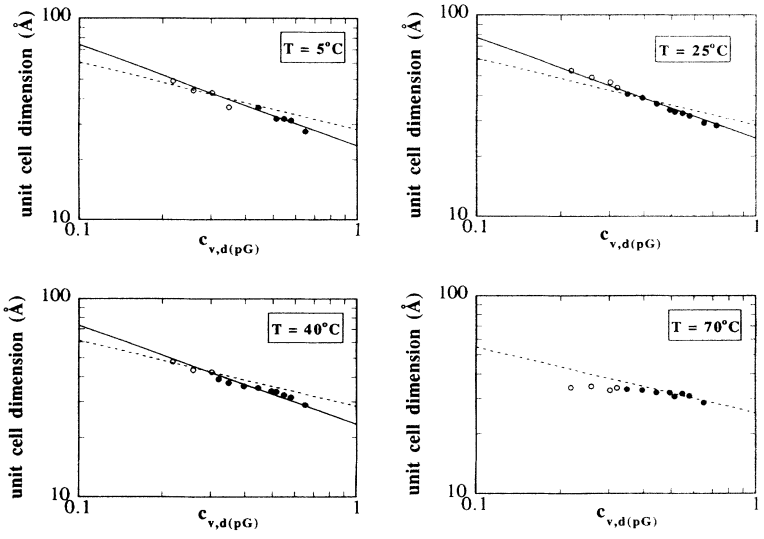

FIG. 4. Dimension of the hexagonal unit cell a (closed circles) and distance between columns in the cholesteric phase (open circles), calculated from the position of the low-angle peaks, as a function of the volume concentration c_v of d(pG) for different temperatures. The absolute errors on the data for the hexagonal and cholesteric phases are ±1 Å and ±3 Å, respectively. The straight lines represent fits to the data using the power law with exponents $-\frac{1}{2}$ (solid) and $-\frac{1}{3}$ (broken), respectively.

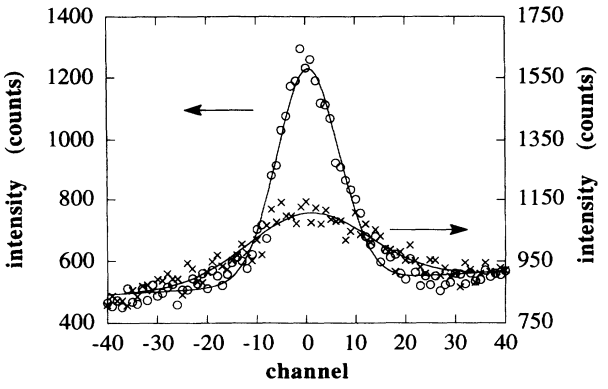

FIG. 5. Diffraction peak centered at $s=(3.4\ \text{Å})^{-1}$ for two different "extreme" cases. ○: $c=50\%$, 35 °C; ×: $c=23\%$, 25 °C. The solid lines represent the Gaussians fitted to the data. For a better comparison, the curves are shifted with respect to each other (note different scales). The full widths at half maximum (FWHM) are 15.0 and 25.4 channels, respectively.

of the peaks—that is four times the scattering angle θ—as a function of concentration and temperature for both investigated systems. In spite of the fact that there is considerable scatter in the data (mainly due to instabilities in the detector electronics), a general trend to increase the distance of the tetramers with increasing temperature is obvious. The corresponding average thermal expansion coefficient was determined to be 0.0013(4) Å/K. The dependence of the full width at half maximum (FWHM) of the $(3.4\ \text{Å})^{-1}$ peak on temperature and concentration is plotted in Fig. 7.

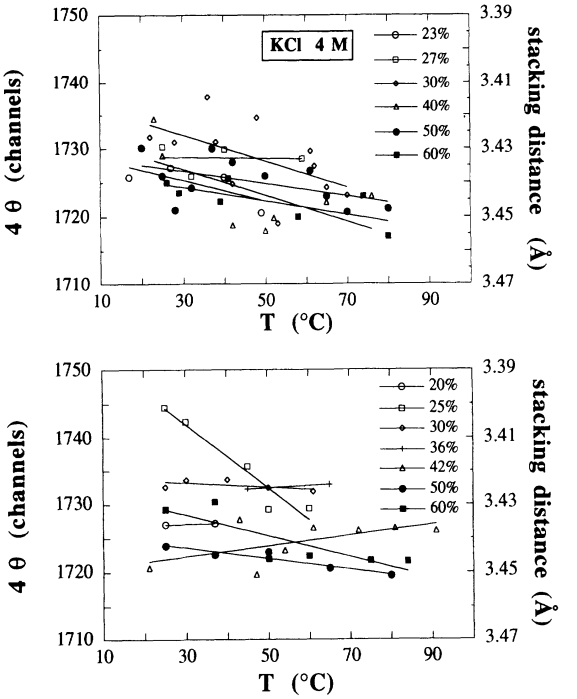

FIG. 6. Distance between the positions of the two high-angle peaks *versus* temperature for different concentrations (as indicated in the figure) of d(pG) in H_2O (lower frame) and 4*M* KCl (upper frame). The scale on the left side is the distance between the position of the peaks for positive and negative scattering angle in channels; in the right scale the scattering angle is converted to the stacking distance. Error bars are omitted for clarity: however, the absolute error in the stacking distance is estimated to be ±0.01 Å. The lines are linear fits to the data to show the general trend.

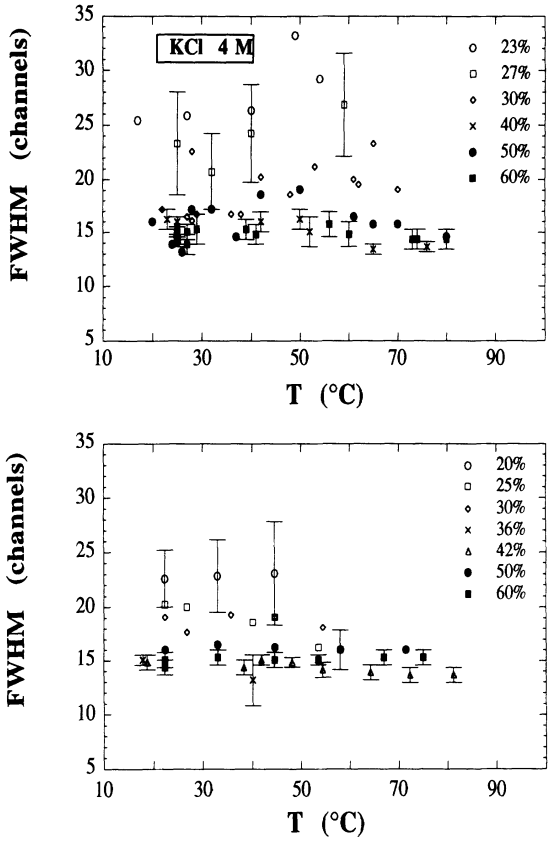

FIG. 7. Full widths at half maximum (FWHM) of the high-angle peak *versus* temperature for different concentrations of d(pG) in H_2O (lower frame) and 4*M* KCl (upper frame). Error bars are omitted in some cases for clarity, but have similar size: in particular, the relative error in the hexagonal and cholesteric phases has been estimated to be about 5% and 20%, respectively.

As already pointed out by Azaroff [26], the Bragg equation must be used with care if the distance between molecules in a liquid crystalline phase is to be determined. To verify the relation between the tetramer stacking distance and the position of the peak in the x-ray diffraction profiles, but also in order to obtain information on the correlation between the changes observed in the peak width and the average number of stacked tetramers, numerical simulations of the SCS of a columnar aggregate have been performed.

To calculate the SCS, the tetramers were approximated by homogeneous disks of 2.35 Å thickness and 13 Å radius [13,15,24]. The scattering amplitude of a given number n of those disks, stacked one above the other at a distance of 3.4 Å, was summed up, squared, and then averaged over all orientations. A random fluctuation of the repeat distance could be accounted for. As expected, this type of disorder has no influence on the width of the

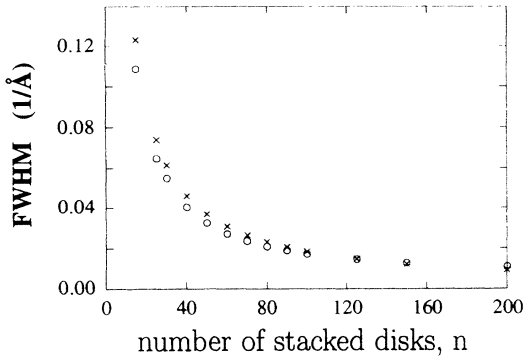

FIG. 8. Calculated full widths at half maximum (FWHM) of the diffraction peak of a stack of n disks (see the text). ×: FWHM calculated using the Scherrer equation; ○: FWHM calculated using the simulation described in the text.

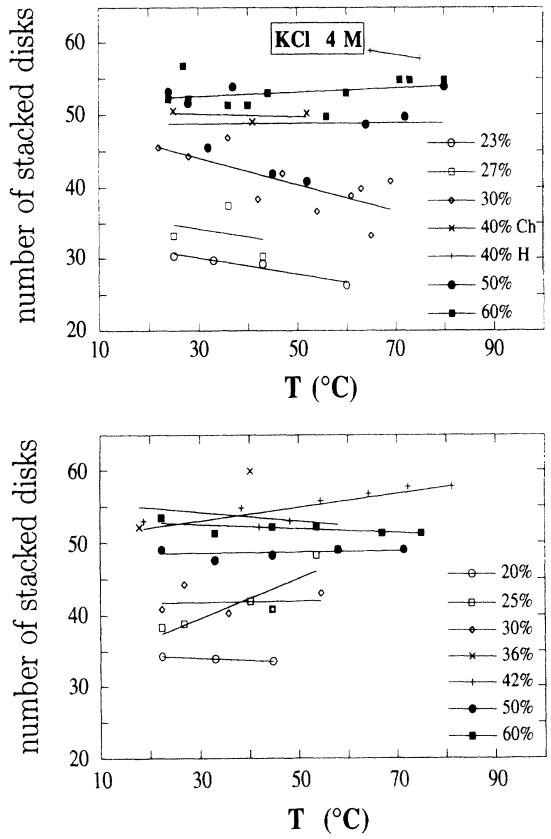

FIG. 9. Average number of stacked disks n, determined by comparing the measured FWHM of the high-angle diffraction peak to the simulated peak width, as a function of temperature in H_2O (lower frame) and 4M KCl (upper frame). Error bars are omitted for clarity: however, in the cholesteric phase the absolute error in the average number of stacked disks is ±8, while in the hexagonal phase the absolute error is ±3. The lines are linear fits to the data to show the general trend. The data belonging to $c=0.4$ are separated into a hexagonal and a cholesteric part.

diffraction peaks. This procedure is correct, as long as there is no three-dimensional correlation between the positions of tetramers in the different aggregates. In Fig. 8, the FWHM of the simulated peaks is plotted as a function of the number of stacked disks n. For short aggregates ($n < 100$) we find a clear deviation from the peak width calculated by using the Scherrer equation [27], whereas for $n > 100$ the agreement is very good. On the other hand, the peak position corresponds always to the value obtained by the Bragg equation (except for very small deviations for $n < 50$).

Therefore, by comparing the calculated and the measured peak width and considering the stacking repeat distance, the average number of stacked disks and the average length of the columnar aggregates have been obtained. The results are reported as a function of concentration and temperature in Fig. 9. It appears evident that the size of the aggregates is not a monotonic function of temperature and that the average correlation length increases as a function of concentration from about 100 Å to 150 Å in the cholesteric phase, but it remains fairly constant (about 170 Å) in the hexagonal domain. This complex dependence will be discussed in the following section.

It may be observed that the value of n determined in this way has to be taken as an average value, because some polydispersity has to be expected in this system. At all concentrations and temperatures investigated, the observed x-ray diffraction high-angle peak could be perfectly fitted with a single Gaussian, indicating that polydispersity is rather small and that the length distribution is symmetric. However, to the degree of experimental accuracy, the polydispersity may not be treated in a quantitative manner, as different curves could be also used to fit the $(3.4\ \text{Å})^{-1}$ Bragg peak within the experimental errors. It may be stressed, however, that simulations clearly indicate that an exponential number length distribution can be excluded. Therefore, we can suggest that the self-assembling process is kinetically controlled [28].

IV. DISCUSSION

In this paper we extended our previous work on the polymorphism of d(pG) at room temperature [13]: the structural properties of the d(pG)-water system have been investigated as a function of temperature and also in the presence of 4M KCl. As a general result, it could be underlined that the microscopic columnar model of stacked tetramers as shown in Fig. 1 agrees with the x-ray data presented. In addition to the analysis of the variation of lateral intercolumnar distance with concentration (Fig. 4), we have also determined the average number of stacked tetramers n, that is the average length L of the columnar aggregates (Fig. 9). Figure 10 shows such data plotted in a different way: the main feature is that the aggregates are relatively short and that their length is comparable to the 65 Å height of the cylindrical particles detected in the isotropic solution by small-angle neutron scattering [15]. Comparing Figs. 9 and 10, it is obvious that L remains approximately constant in the H phase.

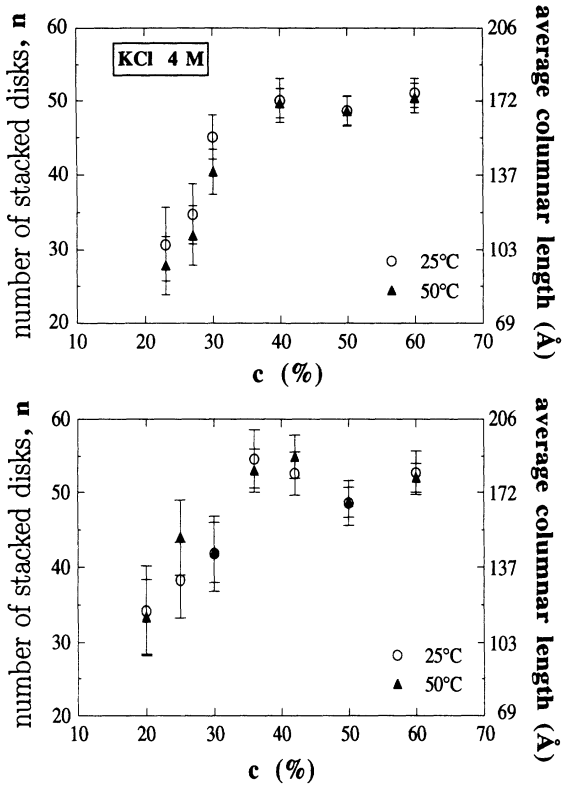

FIG. 10. Average number of stacked disks n as a function of concentration for different temperatures in H_2O (lower frame) and 4M KCl (upper frame). On the right side, the average columnar length, calculated by multiplying the number n by the constant value of 3.43 Å, has also been reported. The Ch to H phase transition occurs at about $c=0.40$.

In contrast, in the Ch phase the aggregates grow in length with increasing concentration and with decreasing temperature. Noticeable is the fact that the phase diagrams derived in [20] and [21] using a hard particle potential surrounded by a weak, short-range repulsive step potential are in good agreement with our findings.

According to our results, the H phase is then formed by columns of stacked disks of radius R and average length L. If the center-to-center distance along the cylinder axis C is written as $C=L+\Delta$, the end-to-end distance between the two aggregates Δ reads as

$$\Delta=L\left[\frac{2\pi R^2}{\sqrt{3}c_v a^2}-1\right].$$

Figure 11 shows the end-to-end distances calculated using $R=13$ Å from the data reported in Fig. 4. As L was found to be approximately constant in the H phase, Δ may be converted to absolute unit using the data of Fig. 9. For low temperatures, the end-to-end distance is approximately 9 Å—independent of concentration—while for high temperatures, Δ increases depending on the concentration up to 60 Å (35% of L). Note that the two points with the highest values of Δ in Fig. 11 are related to the region of phase coexistence, so that the as-

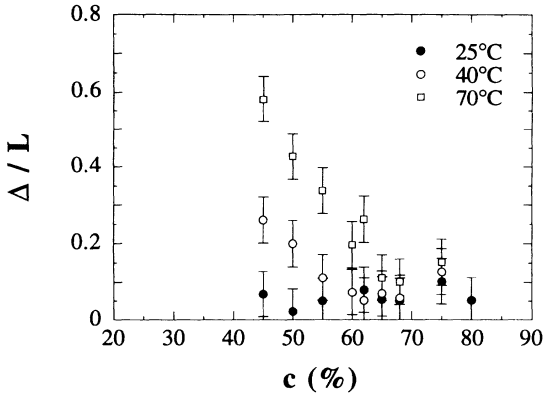

FIG. 11. Axial end-to-end distance Δ between cylinders in the hexagonal phase *versus* the weight concentration of d(pG) for different temperatures. The distance Δ is plotted in units of the cylinder length L.

sumption that the concentration of water in the hexagonal phase is equal to the sample concentration could be no longer valid. Note also that the end-to-end distance must not be regarded as thickness of a water layer, like in a smectic phase, because there is no correlation between the position of the columns in the axial direction.

Interpreting those data, we arrive at the following model for the d(pG) columnar polymorphism. Starting from high concentrations, at low temperature the added water mainly increases the lateral distance between the cylinders, at the expense of the end-to-end separation which remains constant. The aggregates have a well defined length. Nevertheless, as the axial distance is fairly small and constant, they behave like "infinite" objects, longer than the flexibility persistence length. As dilution proceeds, the lattice parameter increases (with exponent $-\frac{1}{2}$) until the hexagonal packing turns unstable relative to the Ch phase. The maximum value of $a/2R$ turned out to be 1.4. In contrast, in the cholesteric phase, the average length of the aggregates decreases with decreasing concentration and with increasing temperature.

At high temperature, the columns are indeed finite "rigid" objects, as though L is unchanged with respect to the low temperature case. In fact, even if the flexibility is expected to increase with temperature [21,25], dilution now mainly determines an increase of the end-to-end distance, so that the aggregate length is smaller than the persistence length. As a consequence, the increase of a is much slower (exponent $-\frac{1}{3}$). However, the aggregation is weak: as the average aggregate size is small, the cholesteric phase disappears. To reach the point of instability versus the Ch phase, a higher quantity of water is needed. But the end-to-end axial separation has already increased up to 35% of the length, resulting in a very loose packing, so that there is a direct transition to the isotropic phase.

By increasing the ionic strength of the solution, we observed a stabilization of the liquid crystalline phase possessing higher symmetry. This stabilization is accompanied by an increase in the two-dimensional hexagonal lattice parameter, whereas the number of stacked tetra-

mers, i.e., the average length of the aggregates, remains constant within the experimental errors. As a consequence, the end-to-end distance Δ between the aggregates is strongly reduced. For example, at a concentration of 50%, the value of Δ in KCl is 13% of L, compared to 30% in pure water. In this condition, the aggregates remain sufficiently elongated, so that the phase boundaries shift to lower concentration, as one might expect in analogy to theoretical results [21]. Both cholesteric and hexagonal phases are more stable: however, as before, the increase of the end-to-end distance observed at high temperature, resulting in a small average elongation of the aggregate, determines the disappearance of the cholesteric phase.

The effect of 4M KCl may be attributed to a specific interaction of K^+ ions, which have the appropriate size to keep together two tetrameric planes *via* coordination with the eight oxygens of the guanine moiety, so that the rods move apart mainly laterally as dilution proceeds. According to what was observed in charged lipid systems [29,30], the decrease of the water activity might also be taken into account, as it will influence the building up of the hydration shell. Therefore, the modified balance between hydration repulsion and solvent-structure-mediated attraction [29,31] between charged cylinders could push them apart. Yet the interplay between ions, the hydration shell, and charged phosphate groups remains to be fully investigated.

Our data indicate that the distribution of water in the hexagonal phase is determined mainly by the lateral interaction between the columnar aggregates. The temperature dependence of the hexagonal cell dimension and the high temperature phase behavior, however, show also that axial interactions, mediated by the presence of ions and maybe by correlated water, play an important role. The results indicate that d(pG) aggregates, which are short in length, are also rather straight and rigid, confirming that flexibility may significantly influence the relative stability of mesophases only for long aggregates, i.e., when the aggregation is strong [24]. Further work will have to concentrate on the dynamics of these columnar aggregates in order to obtain more information on the microscopic nature of these interactions.

Note added in proof. Very recently theoretical and experimental results clearly demonstrate that the exponent in the power-law dependence for the variation of the dimensions of the hexagonal unit cell with volume concentration for monodisperse rigid spherocylinders that grow in length with concentration (see Sec. III B) must be greater than $-\frac{1}{3}$ [P. Mariani and L. Q. Amaral, Phys. Rev. E (to be published)].

ACKNOWLEDGMENTS

We would like to thank G. Gottarelli and G. P. Spada for many helpful conversations. One of us (H.F.) would like to acknowledge the support of the European Community under Contract No. ERBCHBGCT920204. This work was partially financed by MURST and CNR (Italy).

[1] M. Gellert, M. N. Lipsett, and D. R. Davis, Proc. Natl. Acad. Sci. U.S.A. **48**, 2013 (1962).
[2] S. Arnott, R. Chandrasekaran, and C. M. Marttila, Biochem. J. **141**, 537 (1974).
[3] S. B. Zimmerman, J. Mol. Biol. **106**, 663 (1976).
[4] W. Saenger, *Principles of Nucleic Acid Structure* (Springer-Verlag, Berlin, 1984), p. 315.
[5] K. Hoogsteen, Acta Crystallogr. **12**, 822 (1959).
[6] D. Sen and W. Gilbert, Curr. Opin. Struct. Biol. **1**, 435 (1991).
[7] W. I. Sundquist and A. Klug, Nature **342**, 825 (1989).
[8] D. Sen and W. Gilbert, Nature **334**, 364 (1988).
[9] D. Sen and W. Gilbert, Biochem. **31**, 65 (1992).
[10] C. Detellier and P. Laslo, J. Am. Chem. Soc. **102**, 1135 (1980).
[11] G. P. Spada, A. Carcuro, F. P. Colonna, A. Garbesi, and G. Gottarelli, Liq. Cryst. **3**, 651 (1988).
[12] P. Mariani, C. Mazabard, A. Garbesi, and G. P. Spada, J. Am. Chem. Soc. **111**, 6369 (1989).
[13] S. Bonazzi, M. Capobianco, M. M. De Morais, A. Garbesi, G. Gottarelli, P. Mariani, M. G. Ponzi Bossi, G. P. Spada, and L. Tondelli, J. Am. Chem. Soc. **113**, 5809 (1991).
[14] L. Q. Amaral, R. Itri, P. Mariani, and R. Micheletto, Liq. Cryst. **12**, 913 (1992).
[15] F. Carsughi, M. Ceretti, and P. Mariani, Eur. Biophys. J. **21**, 155 (1992).
[16] P. Mariani, M. M. De Morais, G. Gottarelli, G. P. Spada, H. Delacroix, and L. Tondelli, Liq. Cryst. **15**, 757 (1993).
[17] D. Sen and W. Gilbert, Nature **344**, 825 (1989).
[18] M. K. Raghuraman and T. R. Cech, Nucleic Acids Res. **18**, 154 543 (1990).
[19] G. Gottarelli and G. P. Spada (unpublished).
[20] M. P. Taylor and J. Herzfeld, Phys. Rev. A **43**, 1892 (1991).
[21] R. Hentschke and J. Herzfeld, Phys. Rev. A **44**, 1148 (1991).
[22] L. Q. Amaral, A. Gulik, R. Itri, and P. Mariani, Phys. Rev. A **46**, 3548 (1992).
[23] V. Luzzati, in *Biological Membranes,* edited by D. Chapman (Academic, London, 1968), Chap. 3.
[24] C. L. Fisk, E. D. Becker, H. T. Miles, and T. J. Pinnavaia, J. Am. Chem. Soc. **104**, 3307 (1982).
[25] R. Hentschke, Liq. Cryst. **10**, 691 (1991).
[26] L. V. Azaroff, Mol. Cryst. Liq. Cryst. **60**, 73 (1980).
[27] See, for example, H. P. Klug and L. E. Alexander, *X-ray Diffraction Procedures* (Wiley, New York, 1974).
[28] See, for example, W. Hoppe, W. Lohmann, H. Markl, and H. Ziegler, *Biophysik* (Springer-Verlag, Berlin, 1982).
[29] R. P. Rand and V. A. Parsegian, Biochim. Biophys. Acta **988**, 351 (1989).
[30] J. M. Seddon, Biochim. Biophys. Acta **1031**, 1 (1990).
[31] D. C. Rau, B. Lee, and V. A. Parsegian, Proc. Natl. Acad. Sci. U.S.A. **81**, 2621 (1984).

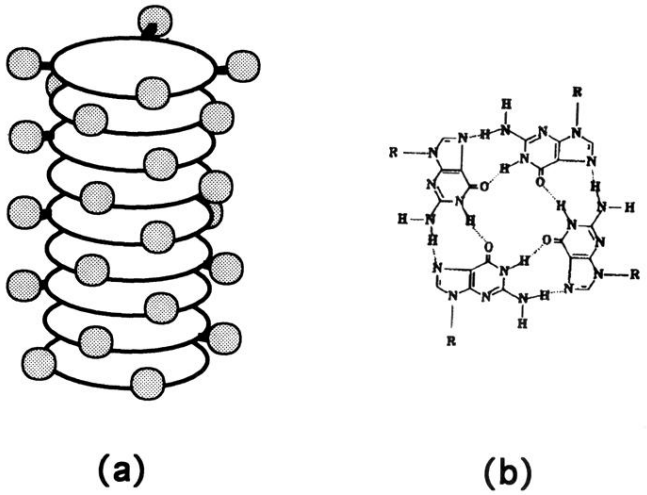

FIG. 1. Schematic representation of the microscopic structure of d(pG) aggregates. (a) Stacking of the disk-shaped tetramers. The spherical legands symbolize the residual sugar groups (R). (b) In-plane structure of one tetramer.

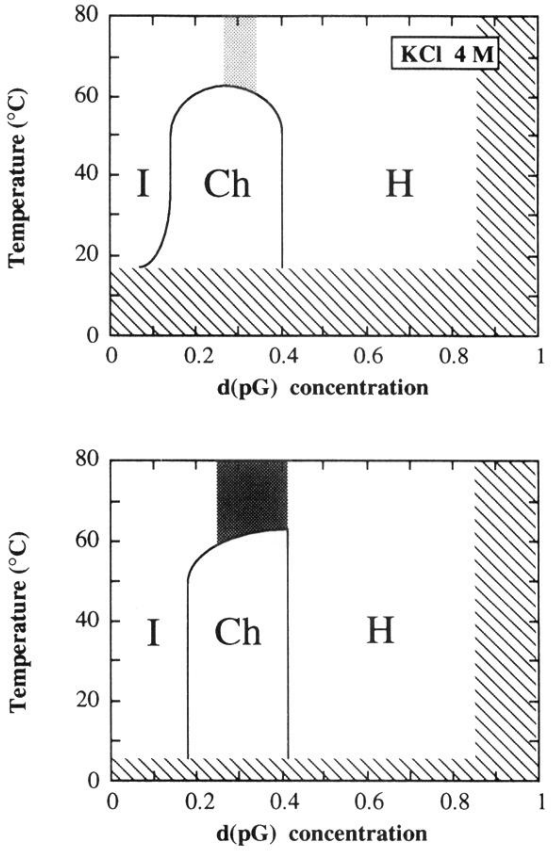

FIG. 3. Phase diagrams of d(pG)-H_2O (lower frame) and d(pG)–4*M* KCl (upper frame) as deduced from our measurements (concentrations in relative weight). *I*, isotropic, Ch, cholesteric, and *H*, hexagonal phases. Shaded region: phase coexistence. The lines give the positions of the phase transitions, the width of which was determined to be below 5%. In the hatched areas, we have no measured data.